Astrophysical light scattering problems (PAP316)

Lecture 3a

Karri Muinonen
Academy Professor
Department of Physics, University of Helsinki, Finland

Contents

- Introduction
- Moon
  - Polarimetry
  - Photometry
  - Spectrometry
- Intermediate conclusions

Introduction

- Physical characterization of astronomical objects (e.g., surfaces of airless planetary objects)
- Direct problem of light scattering by particles with varying particle size, shape, refractive index, and spatial distribution
- Inverse problem based on astronomical observations and/or experimental measurements
- Plane of scattering, scattering angle, solar phase angle, degree of linear polarization

Moon

- Western portion (last quarter) of lunar disk in perpendicular and parallel polarization
- Difference can be visually confirmed

FIGURE 18.1 Images of the lunar last quarter acquired in blue light using a polarizing filter with perpendicular (left) and parallel (right) orientations of the polarization axis.

Data were obtained with a telescope of the Kharkov astronomical observatory.

Polarimetric & photometric observations

Moon

Photometry

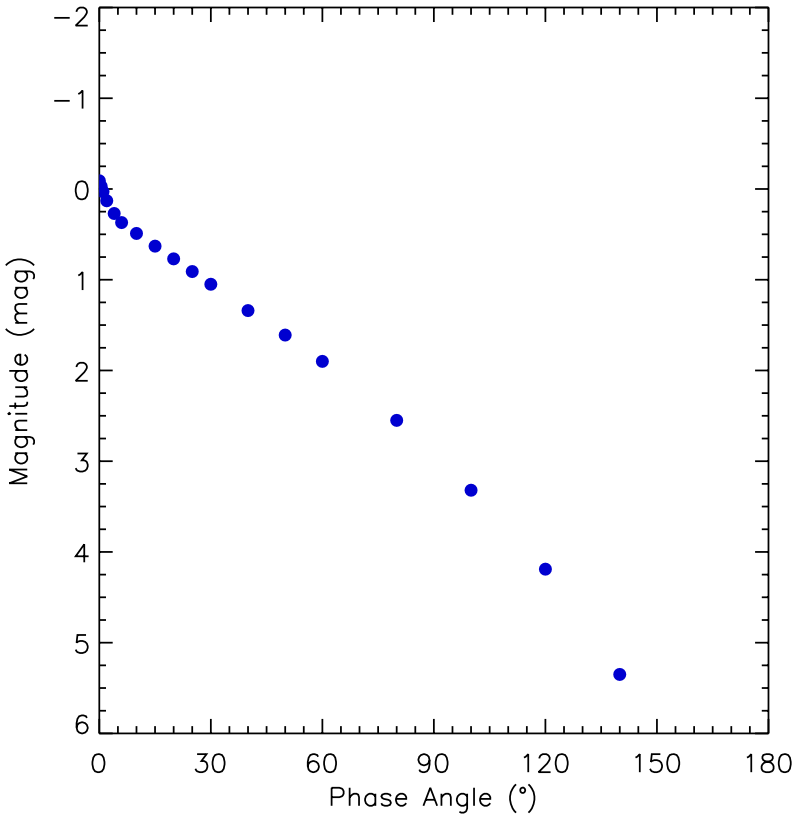

Polarimetry

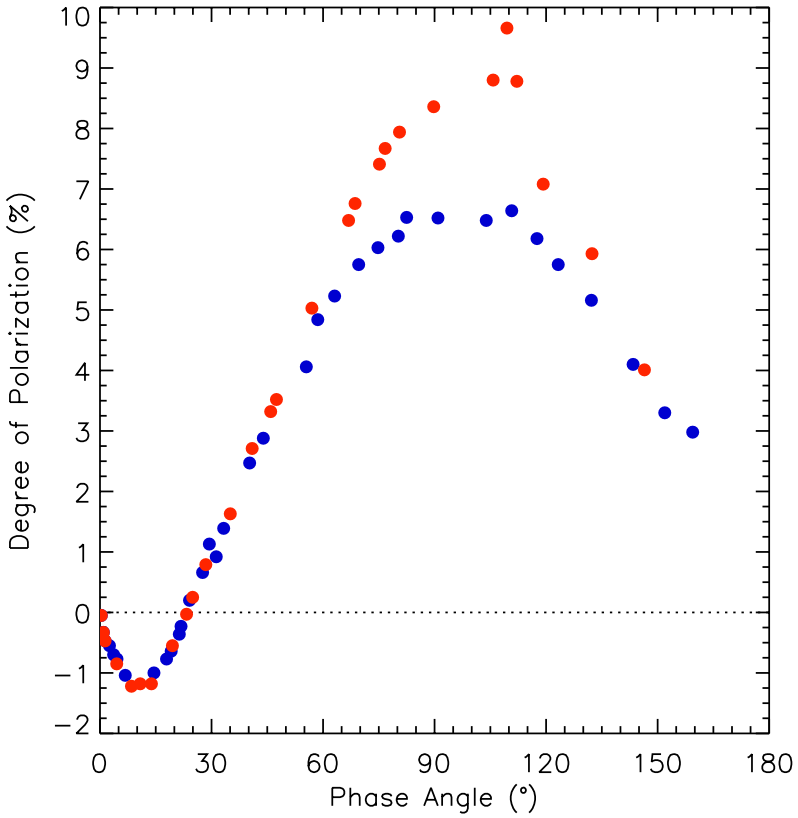

Rougier (1933), Lyot (1929)

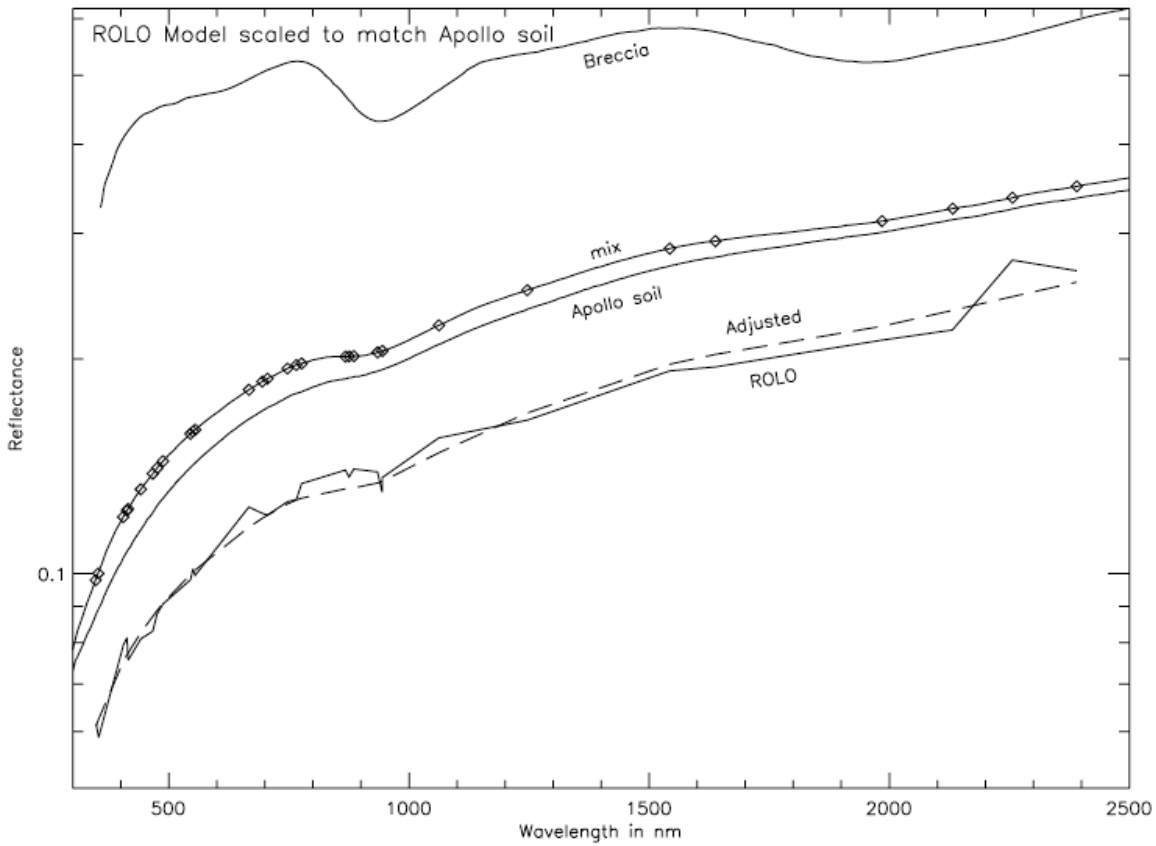

FIG. 8.—Adjustment to the ROLO model reflectance using *Apollo* spectra. The three upper curves are a returned *Apollo* soil sample at 5 nm resolution (*lower solid line*; Pieters 1999), a lunar breccia sample (*upper solid line*; Pieters & Mustard 1988), and a mix with 5% breccia with convolution over the ROLO bands (*diamonds*). The lower jagged line is the unadjusted ROLO model lunar spectrum for 7° phase angle and zero libration. The dashed line is the *Apollo* representative (mixed) spectrum scaled by $a + b\lambda$ to best fit the ROLO spectrum, yielding the 311g model.

Kieffer and Stone, Astron. J. 129, 2887, 2005

- Polarization of Luna 16 landing site at varying phase angle
- Homogeneous sample shows higher maximum polarization
- Six basic polarimetric parameters defined

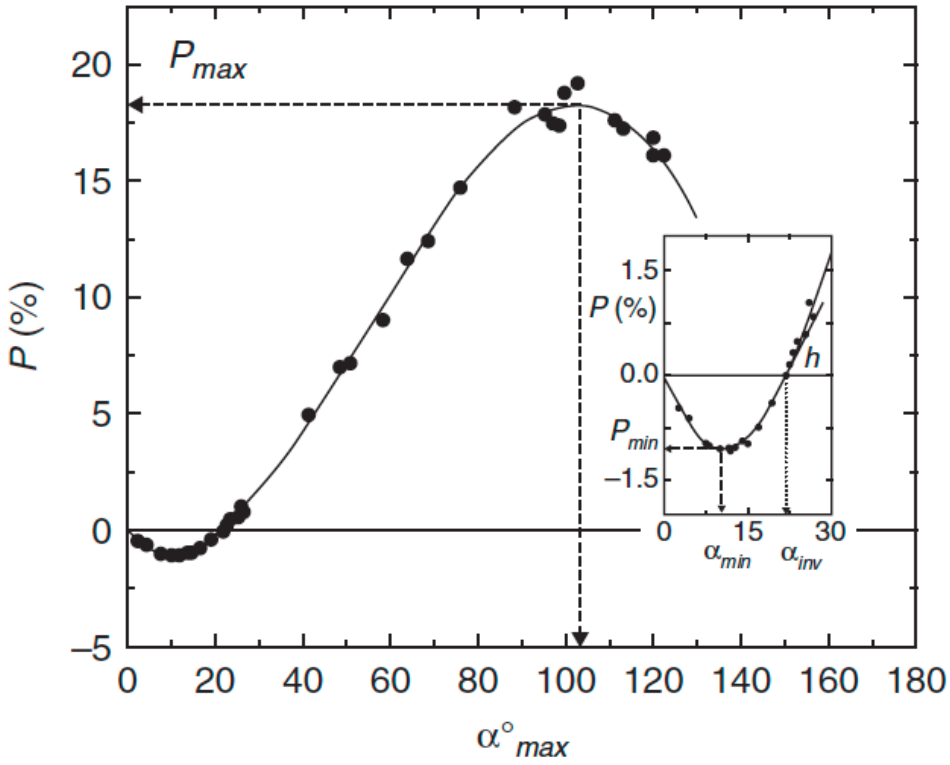

FIGURE 18.2 Polarimetric phase function of the Luna-16 landing site plotted using Kvaratskhelia (1988) data at λ = 0.43 μm. The main six polarimetric parameters are shown.

- Polarization phase curve can be explained by scattering by single particles and coherent backscattering effect in multiple scattering
- Photometric phase curve is additionally influenced by shadowing effects due to large particles

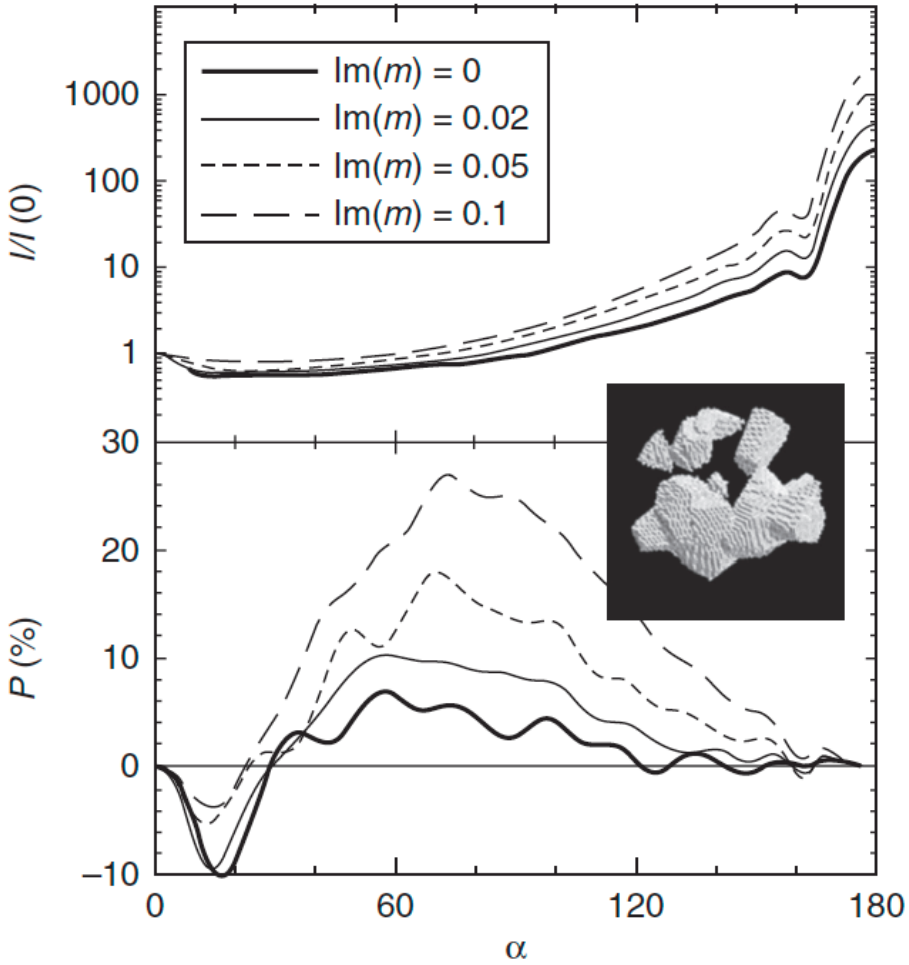

FIGURE 18.3 Phase curves of normalized intensity and linear polarization degree of the agglomerated debris particles for different absorptions (the imaginary part of the refractive index). The size parameter x and the real part of refractive index n are equal to 14 and 1.5, respectively.

Reproduced from Zubko *et al.* (2009) with permission from Elsevier.

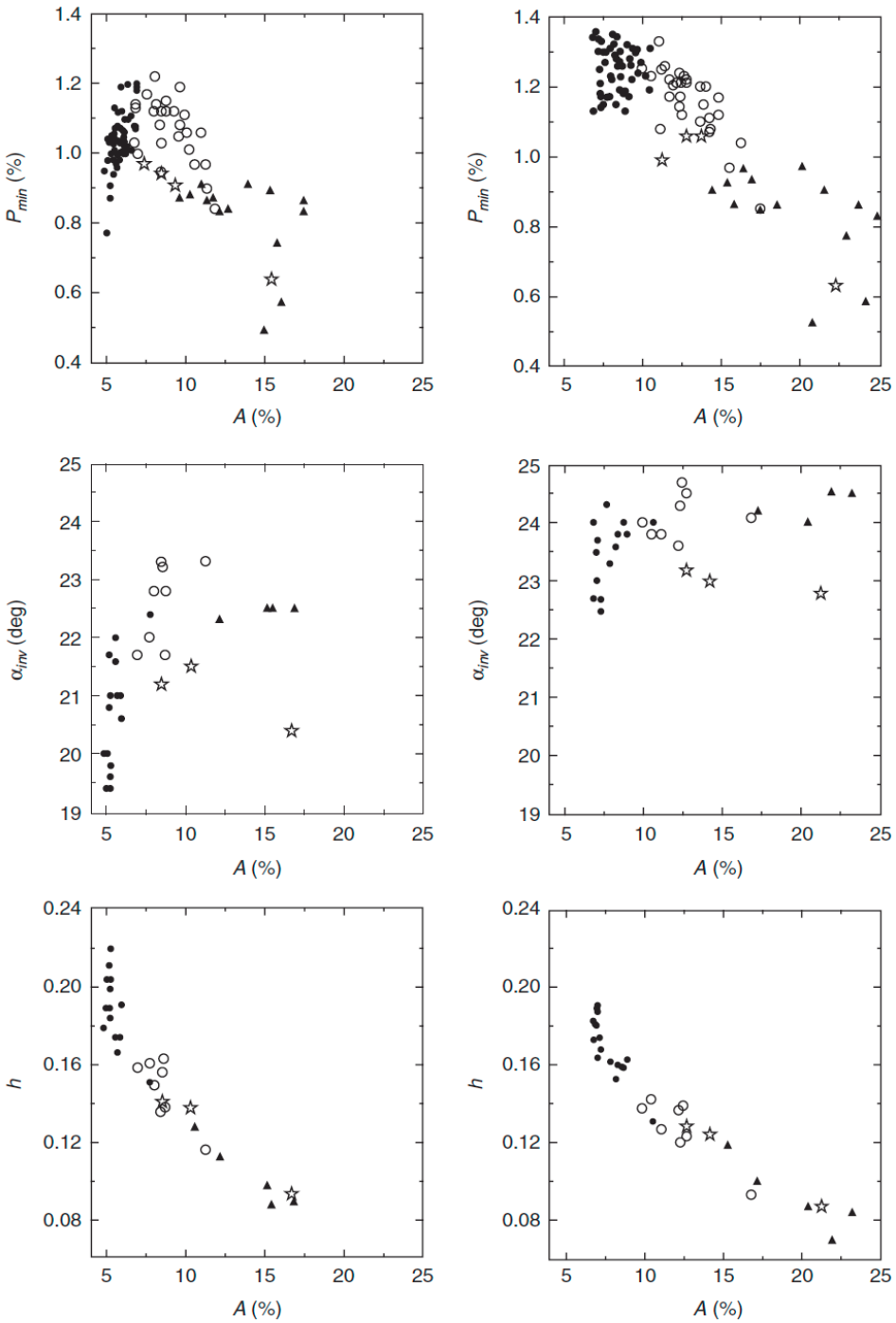

FIGURE 18.4 Correlations of the negative polarization parameters with albedo (based on the data from Shkuratov *et al.* 1992a). The left and right columns correspond to observations at λ = 0.43 and λ = 0.62 μm. Closed and open circles present mare and highland sites, respectively; whereas, stars and triangles correspond to craters.

- Polarimetric parameters against geometric albedo proxy (λ = 430 nm & λ = 620 nm)
- Nonlinear horseshoe shape in P_{min} for 430 nm vs. linear shape for 620 nm

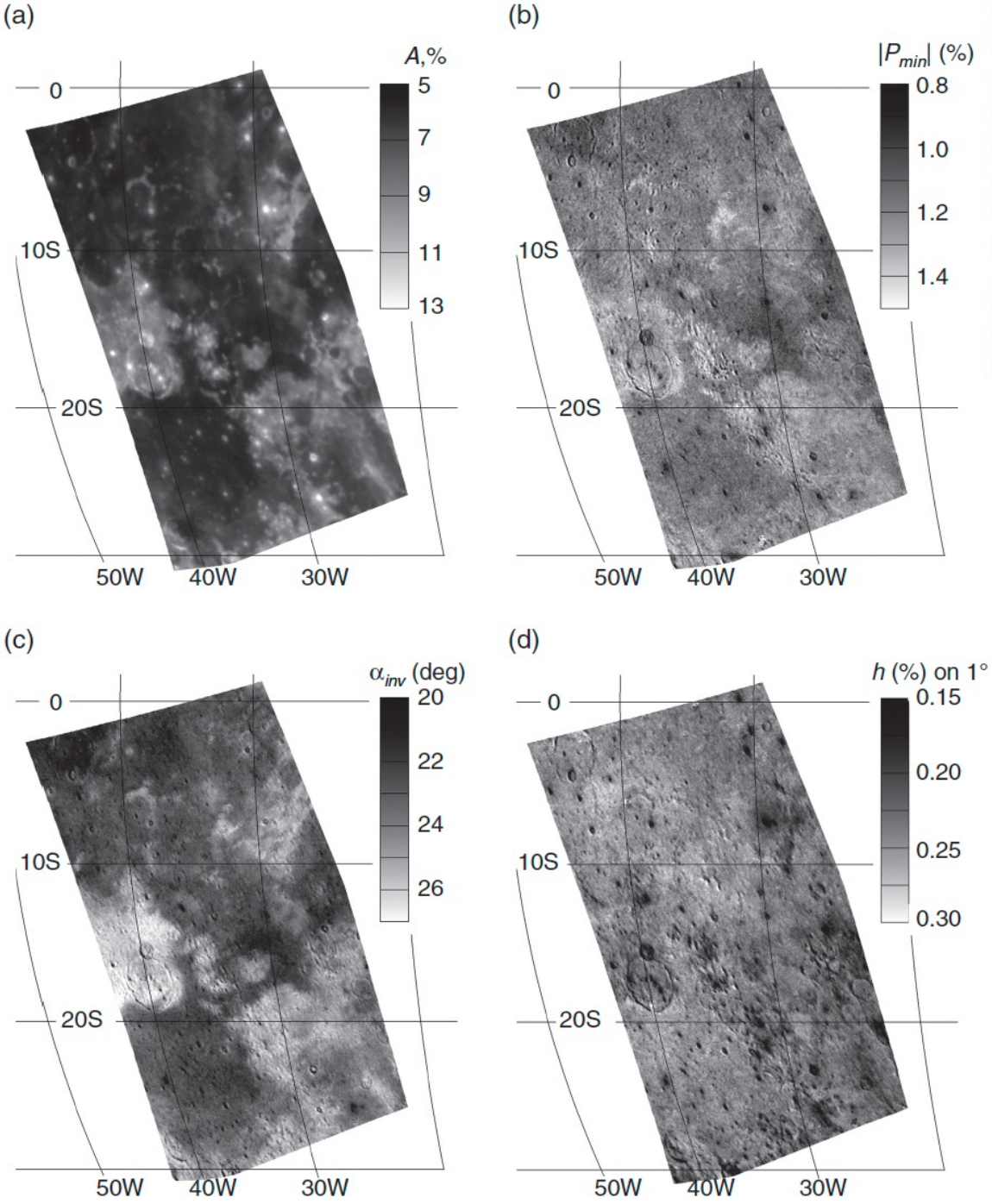

FIGURE 18.5 Polarimetric images of the southwestern portion of Oceanus Procellarum at λ = 0.52 μm. (a) Reflectance; (b) the depth of the polarimetric phase curve at minimum polarization P_{min}; (c) the inversion angle α_{inv}; and (d) the slope h of the polarimetric phase curve at α_{inv}.

Adapted from Shkuratov *et al.* (2011); reproduced with permission from Elsevier.

- Reflectance vs. P_{min} vs. α_{inv} vs. h
- Anticorrelation vs. correlation

- Mosaic image of polarization degree near minimum polarization (520 nm)
- Notice the substantial information content
- Prospects for taxonomical classification!

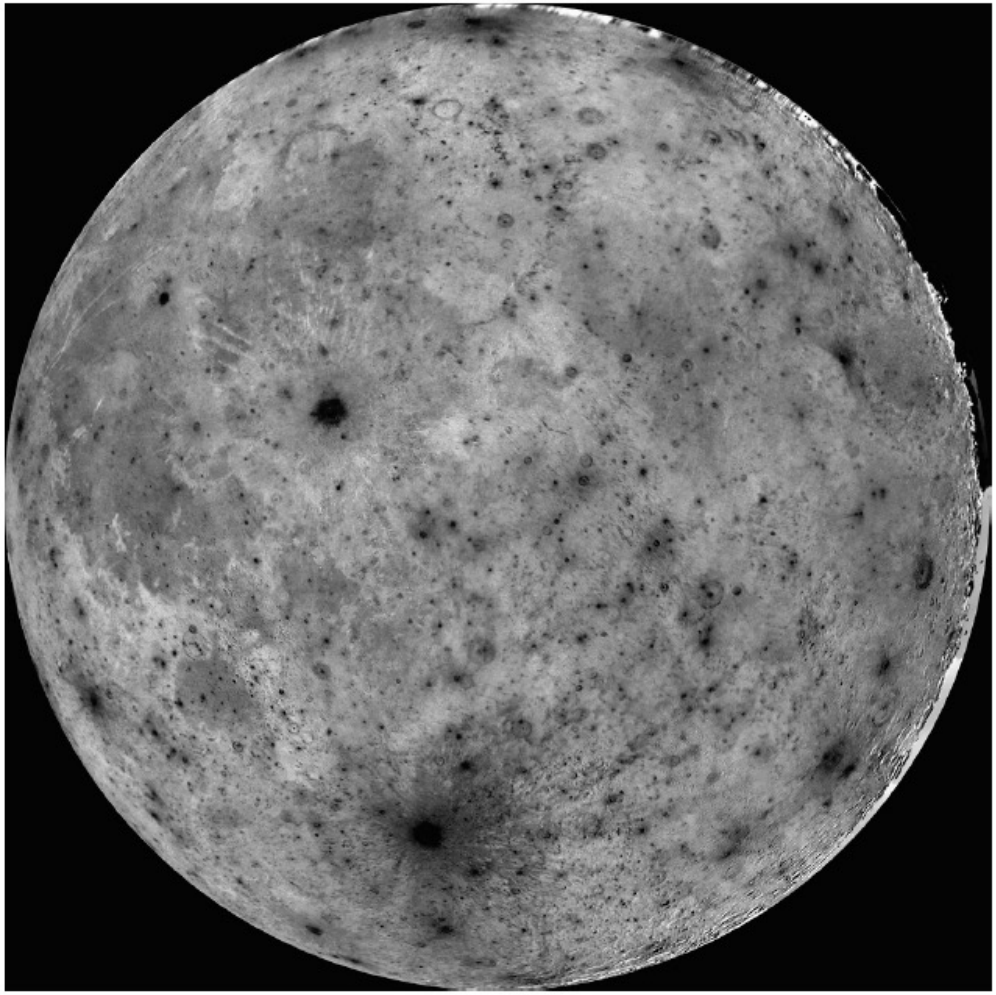

FIGURE 18.6 A mosaic of polarization degree close to P_{min} for the lunar nearside taken at λ = 0.52 μm.

This image was adapted from Opanasenko *et al.* (2013).

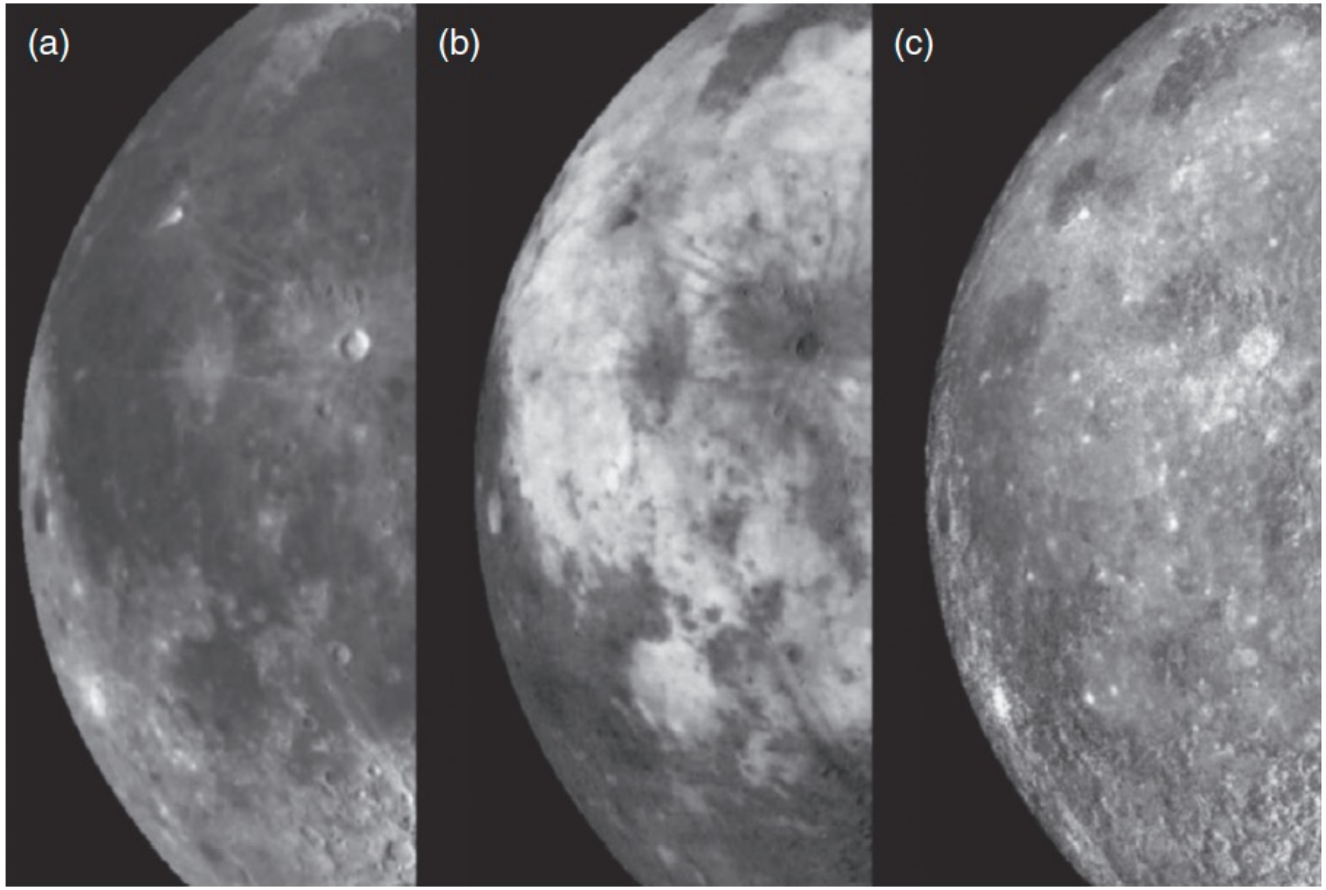

FIGURE 18.7 Earth-based telescope photopolarimetric images of the western portion of the lunar nearside. (a) An equigonal albedo image (after compensation of the global brightness trend from limb to terminator); (b) an image of polarization degree; and (c) an image of deviation from Umov's effect, the parameter $b = A(P_{max})^a$.

Reproduced from Shkuratov *et al.* (2007) with permission of Elsevier.

- Albedo proxy vs. degree of polarization vs. deviation from Umov's law
- Potential for taxonomical classification if only the physical and chemical implications were understood!

- Phase angle α_{max} for red and blue light
- Higher angle for blue light could be understood with less divergent specular reflection lobes (narrower diffraction patterns)

FIGURE 18.8 A distribution of α_{max} for the eastern portion of the lunar disk in (a) red and (b) blue light. The values of α_{max} (degrees) were determined with polarimetric images obtained at ten different phase angles. The parameter scale is common for both images.

Adapted from Korokhin and Velikodsky (2005).

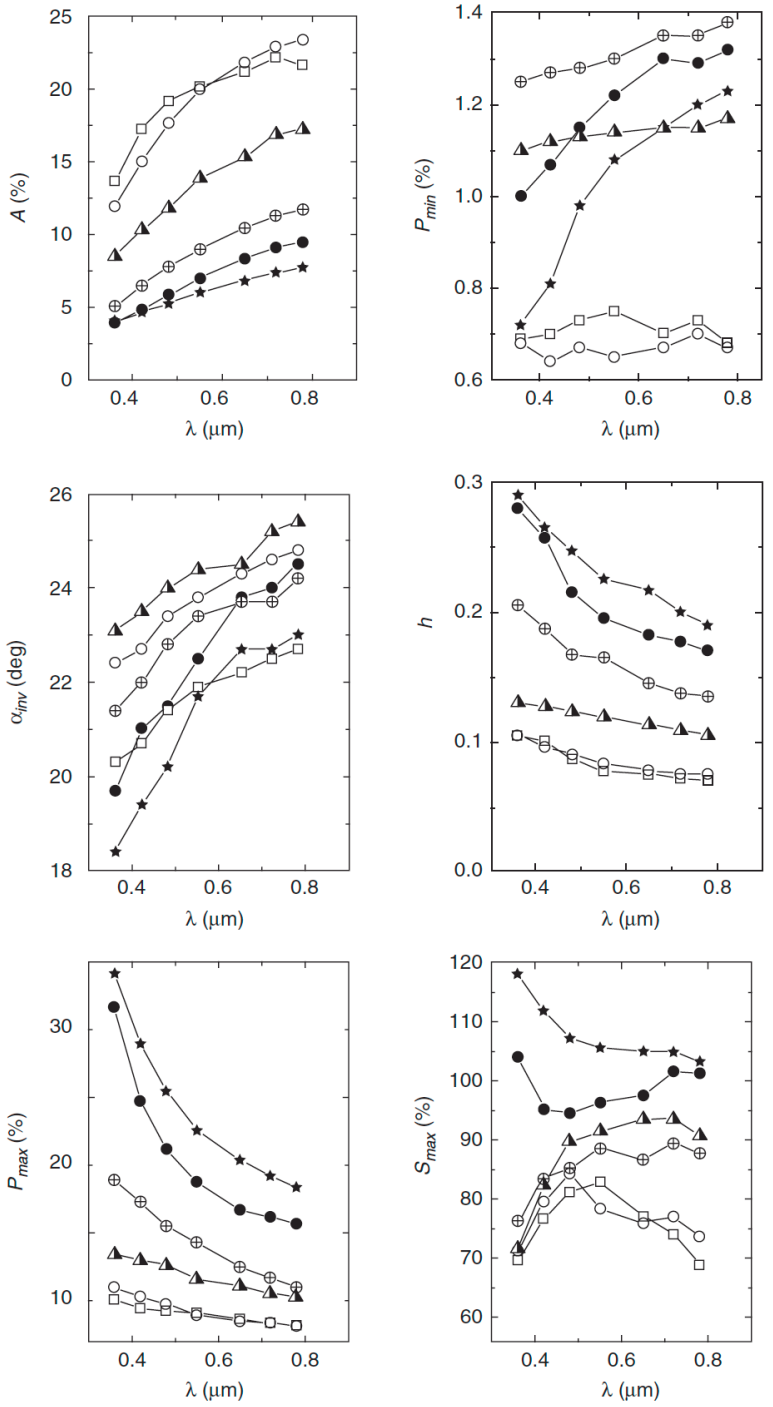

FIGURE 18.9 Spectral dependences of reflectance, $|P_{min}|$, α_{inv}, h, P_{max}, P_{max}, and S_{max} for six lunar sites of different morphological type: symbols 1 and 2 represent young craters Proclus and Aristarchus, 3 and 4 show highlands with intermediate albedo (near crater Newcomb and Helmet), and 5 and 6 correspond to the mare area near crater Flamsteed.

Based on the data from Opanasenko and Shkuratov (1994).

- Spectroscopy vs. P_{min} vs. α_{inv} vs. h vs. P_{max} vs. S_{max} (Stokes Q instead of –Q/I)
- Six lunar sites of different morphological type

- Search for polarization effets in shallow absorption bands
- Four lunar areas: Plato (1), Mare Humorum (2), Helmet (3), Aristarchus (4)

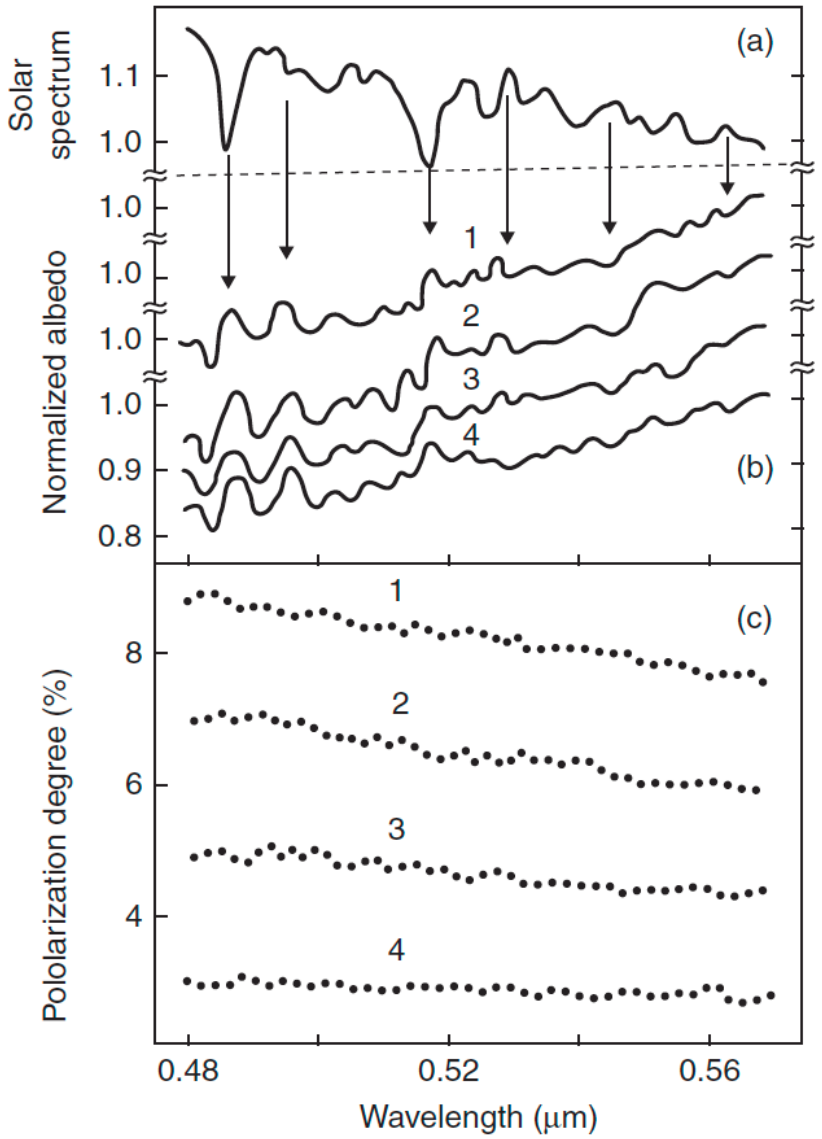

FIGURE 18.10 (a) Solar spectrum, (b) spectral curves of albedo, and (c) polarization degree measured at four lunar areas: curves 1–4 correspond to the crater Plato (center), Mare Humorum, formation Helmet, and crater Aristarchus, respectively.

Based on the data from Opanasenko and Shkuratov (1994).

- Breakdown of Umov's effect at ultraviolet wavelengths
- Polarization degree increases although the geometric albedo flattens out

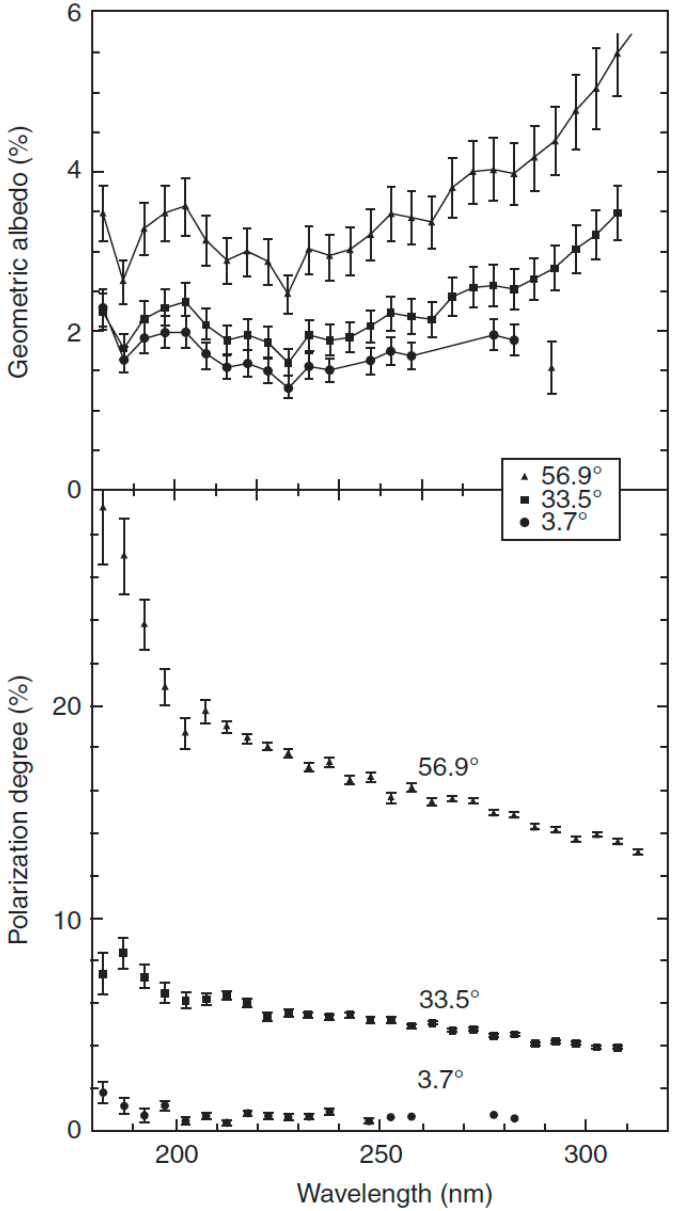

FIGURE 18.11 The variation of the geometric albedo and degree of polarization with wavelength for the three sites observed by WUPPE at a resolution of 50 angstroms. Measured sites at the three indicated phase angles are different.

Reproduced from Fox *et al.* (1998), Figs 1 and 2.

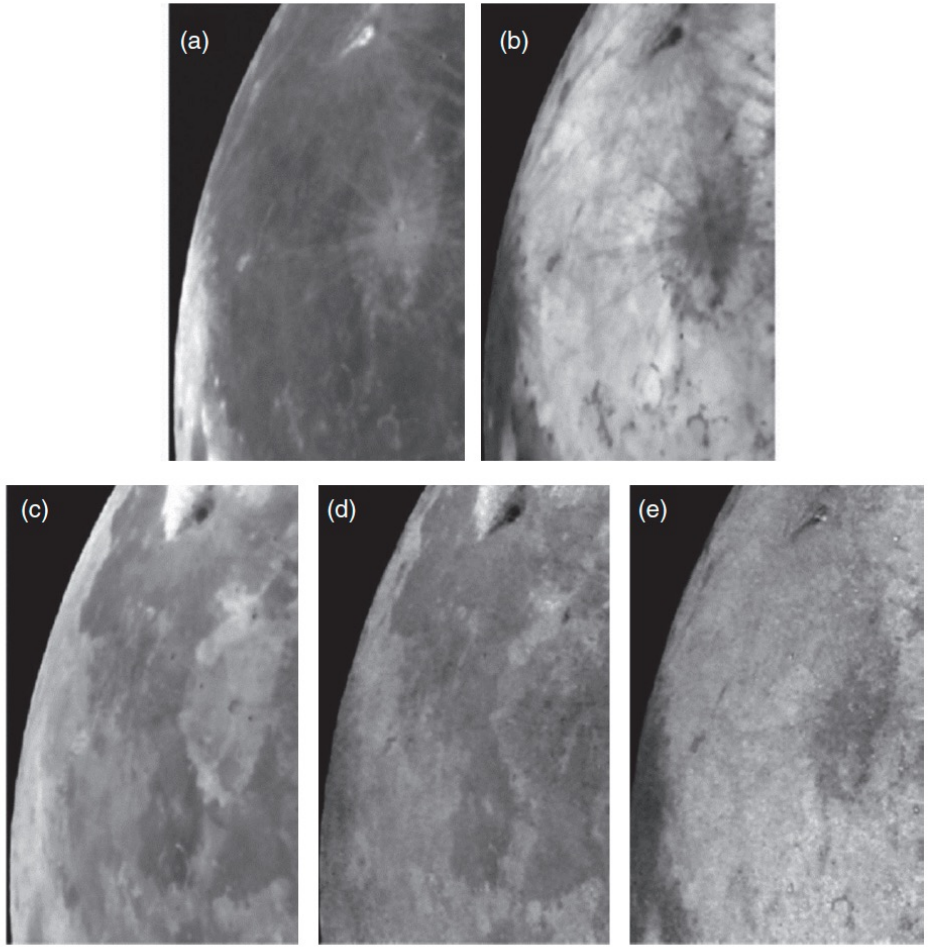

FIGURE 18.12 Photopolarimetric parameters of the northern portion of Oceanus Procellarum at α = 96°: (a) albedo distribution (λ = 0.63 μm); (b) polarization degree distribution (λ = 0.48 μm); (c) color ratio C(0.63/0.48 μm); (d) polarimetric color ratio C_P(0.48/0.63 μm); and (e) color ratio for the second Stokes parameter C_Q(0.48/0.63 μm).

Reproduced from Shkuratov *et al.* (2011) with permission from Elsevier.

- Albedo proxy, degree of polarization, color ratio, and polarimetric color (Q)
- α = 96°

- Degree of polarization and polarization plane orientation
- Plane variations modest

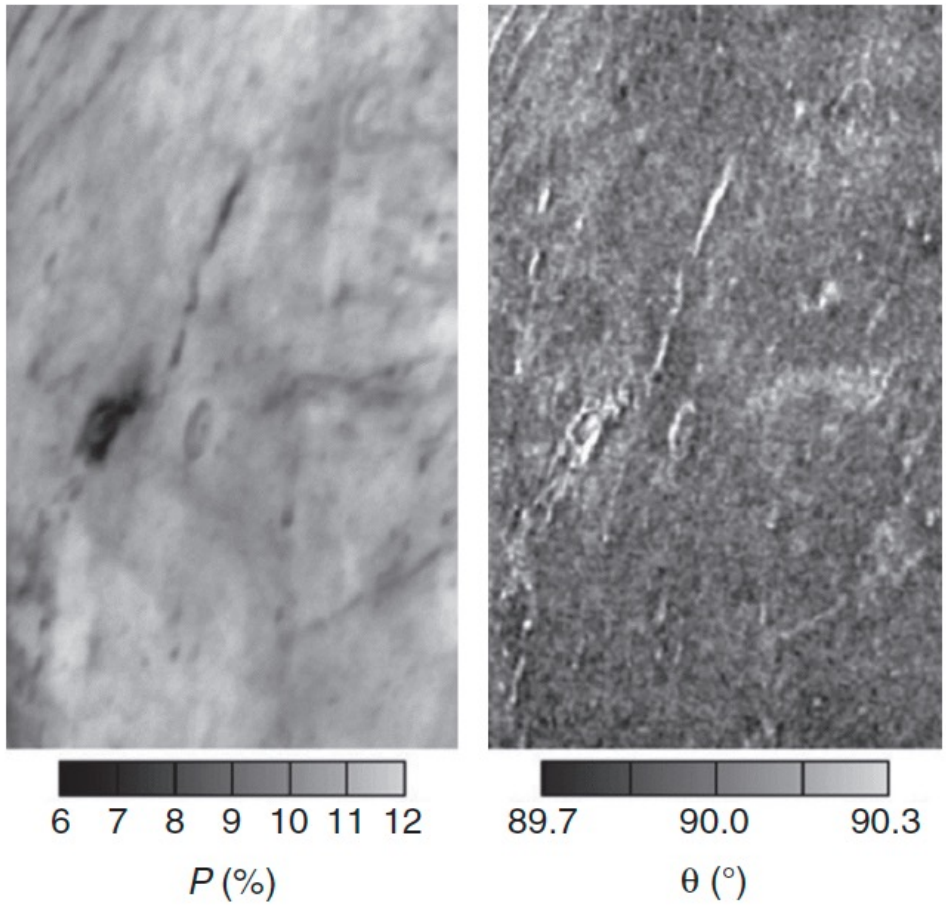

FIGURE 18.13 Images of the central portion of Oceanus Procellarum. Left and right panels correspond to the linear polarization degree and the angle that characterizes the orientation of the polarization plane, respectively.

Reproduced from Shkuratov *et al.* (2011) with permission from Elsevier.

- Polarization degree near α_{inv} for 630 nm and 480 nm
- Dark, intermediate, white tones correspond to negative, positive, and ~zero polarization

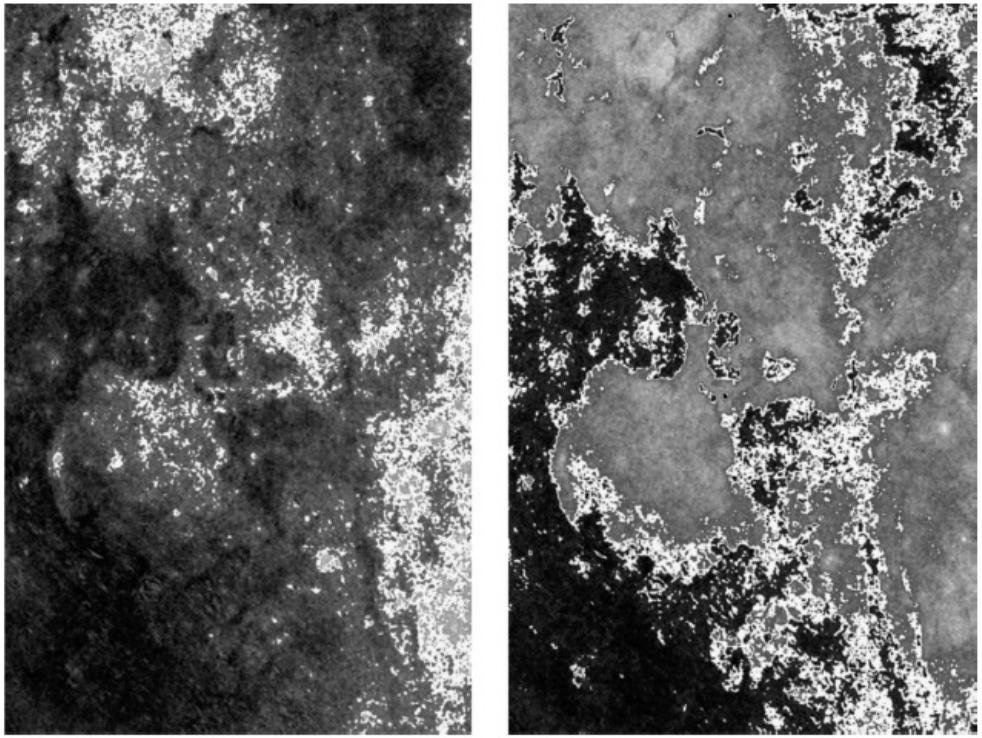

FIGURE 18.14 Images of Mare Humorum and a portion of Oceanus Procellarum. Dark, intermediate, and white tones correspond to the following polarization degree $P < -0.05\%$ (negative), $P > 0.05\%$ (positive), and $-0.05\% < P < 0.05\%$ ("zero" polarization). Left and right images correspond to 0.63 μm and 0.48 μm, respectively.

- Exoplanet research by polarimetric imaging of Earthshine on the Moon
- Lunar regolith Mueller matrix unknown (!) so depolarization properties of the “detector” undefined

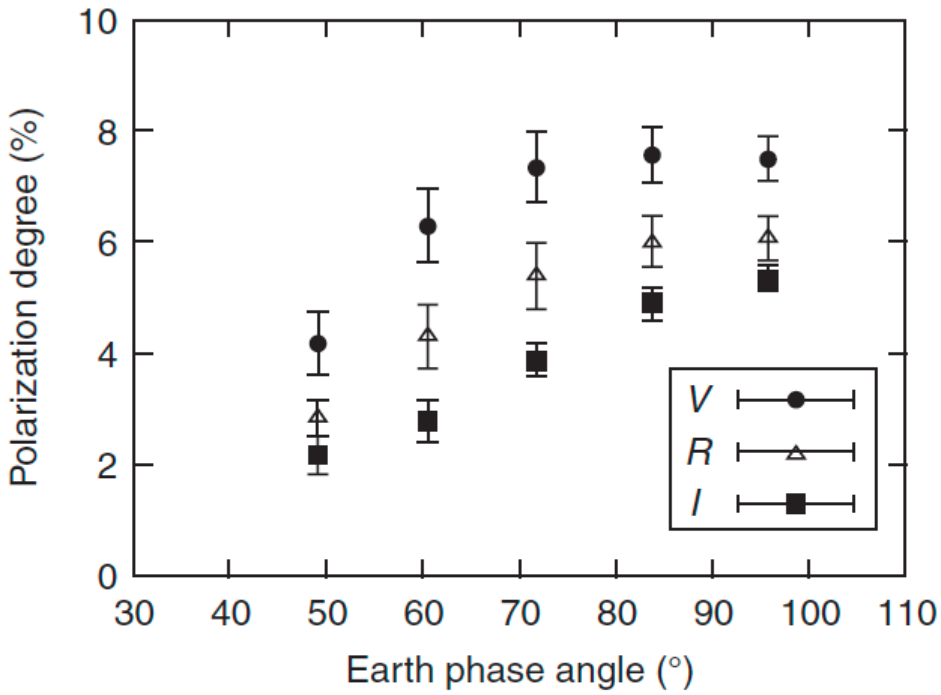

FIGURE 18.15 Earthshine polarization degree as a function of the Earth phase angle, averaged for the V (0.507–0.599 μm), R (0.589–0.727 μm), and I (0.731–0.881 μm) bands.

Based on the data from Takashi *et al.* (2013).

- Polarization of the Moon's ashen light, that is, Earthshine
- Large phase angles of 127^{o} and 161^{o}
- Substantial noise in the image for the larger phase angle

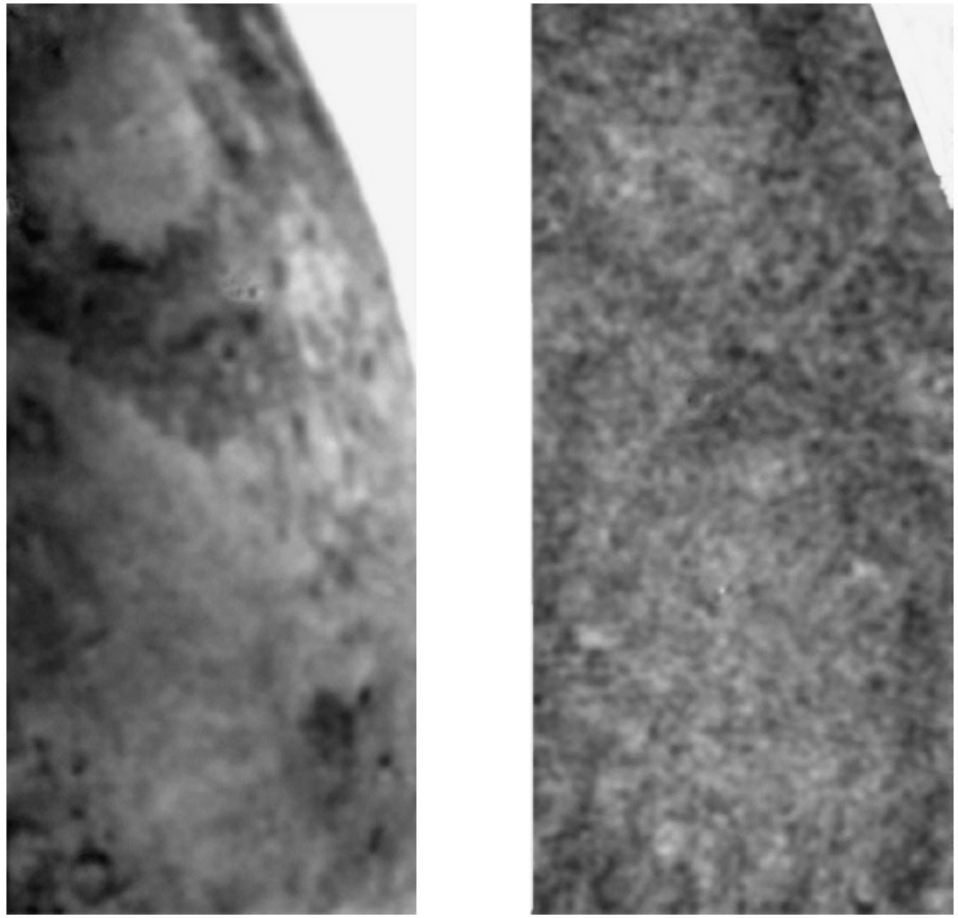

FIGURE 18.16 Polarization of the Earthshine on the eastern edge of the lunar nearside at λ = 0.52 μm. Left and right panels correspond to the lunar phase angle 127° and lunar phase angle 161°, respectively.

Intermediate conclusions

- Lunar surface provides a challenging cosmic laboratory for light scattering
- Earth as an exoplanet can be studied by using the Moon as the “detector”
- Lunar regolith scattering Mueller matrix still an enigma